CONF-780431--6

To be presented at the 3rd Int. Conf on Plasma Surface Interactions in Controlled Fusion Devices, Culham Lab., Abingdon Oxfordshire, U. K., 3-7 April 1978.

78-40

COMPUTER SIMULATION OF THE REFLECTION OF HYDROGEN AND THE SPUTTERING OF HYDROGEN FROM METAL HYDRIDES*

MN ONLY

O. S. Oen† and Mark T. Robinson

Abstract

Reflection of 0.1 to 2 keV H atoms from Ti, Fe and their "metal hydrides", together with the H sputtered from the latter, have been calculated using the binary collision cascade program MARLOWE. The fraction of particles and energy reflected is found to decrease with increasing hydrogen content of the metal hydride and this decrease is independent of the incident ion energy. It is found that the heavy metal atoms of the metal hydride are responsible for the reflection and that most of the sputtering is produced by the reflected ion as it exits through the surface layer. It is also found that tritium ions sputter H from "FeH" much more effectively than H ions sputter T from "FeT".

---

*Research sponsored in part by the Division of Materials Sciences, U. S. Department of Energy under contract W-7405-eng-26 with the Union Carbide Corporation.

†Guest scientist at Max-Planck-Institut für Plasmaphysik, EURATOM Association, D-8046 Garching bei Munchen, Germany. Permanent address: Oak Ridge National Laboratory, Oak Ridge, TN, 37830.

QB.

DISCLAIMER

COMPUTER SIMULATION OF THE REFLECTION OF HYDROGEN AND THE SPUTTERING OF HYDROGEN FROM METAL HYDRIDES

O. S. Oen , Max-Planck-Institut für Plasmaphysik, EURATOM Association
D-8046 Garching bei München, Germany

Mark T. Robinson, Solid State Division, Oak Ridge National Laboratory
P.O. Box X, Oak Ridge, Tennessee 37830 U.S.A.

Introduction

The magnetic confinement of the plasma in present-day tokamak reactors is poor. It is estimated that all plasma particles strike the first wall and recycle back into the plasma several times, on the average, during a single discharge.[1] The hydrogen recycling between the plasma and the first wall therefore plays an important role in the particle and energy balances of the system.[2,3] Some fraction of the hydrogen that strikes the wall is reflected (backscattered) with reduced energy into the plasma. The remainder slows down and comes to rest within the wall. There have been several recent experimental[4-11] and theoretical[12-17] studies of the reflection of hydrogen ions with incident energies of a few keV or less, the energy range most relevant to current fusion needs. Experimentally, one of the biggest problems is the difficulty in detecting low-energy, reflected neutral atoms. Insufficient knowledge of the electronic energy losses for low-energy ions is one of the major obstacles to reliable theoretical calculations. In addition to the hydrogen that is directly reflected from the wall back into the plasma, a fraction of the hydrogen that comes to rest may also re-enter the plasma by either diffusive re-emission[18] or through kinetic ejection by sputtering. The hydrogen implanted within the walls may also change the reflection properties of the wall material. Experiments directed to this question are being done currently.[19] However, to the author's knowledge, no calculations have yet treated the sputtering of the implanted hydrogen or the influence that it may have on the reflection properties of a material. These two topics will be treated in this paper.

Calculational Method

The present work investigates the reflection and the sputtering of hydrogen atoms from solids containing varying amounts of hydrogen. The incident energy of the hydrogen ions ranges from 0.1 to 2 keV. The calculations have been made using the binary collision cascade computer program MARLOWE[20]. Briefly, the projectile ion strikes the target surface and is followed collision by collision until it leaves the surface again (reflected), or until it slows down to an energy below a preset limit (5 eV). In addition to following the incident primary ion, MARLOWE also follows the motion of each hydrogen target atom that receives, in any collision, a kinetic energy that is greater than some threshold energy (chosen as 5 eV for these calculations). The struck target atom is assumed to recoil with the full energy received in the collision (zero binding energy) and is followed collision by collision until it is sputtered or until its energy falls below the preset limit (5 eV). A surface binding energy of zero was assumed for the sputtered particles.

Each collision with a target atom consists of an elastic and an inelastic part. The elastic part is described by classical scattering theory using the Moliere approximation[21] to the Thomas Fermi interatomic potential. The inelastic stopping cross section per atom is described using the sum of a local and a nonlocal loss. The nonlocal loss term is chosen to equal one half of the electronic stopping predicted by Lindhard et al. (LSS)[22]. The local loss term depends on the collision impact parameter and has been discussed in detail previously.[15] For energies above about 1 keV, the local and nonlocal terms are equal and their sum is equal to LSS stopping. For lower energies, the local loss is somewhat less than the nonlocal loss. For a compound target, the electronic stopping power is determined using Bragg's Law. The calculations have been made using MARLOWE to simulate amorphous solids.[15] A typical run consists of following the motion of 1000 or more incident particles and recording the statistical information obtained for the reflected and for the sputtered particles.

Results

Figure 1 shows a comparison of the reflection of H from Ti and the reflection and the sputtering of H from TiH_2 for normally incident H ions of 100 eV. It is noted that both the fraction of incident particles reflected, R_N, and the fraction of incident energy reflected, R_E, are reduced by a factor of about two in going from Ti to TiH_2. The sputtering yield of H from TiH_2, S_N, is about 0.1 and the fraction of incident energy carried away by the sputtered particles, S_E, is less than 0.02. The energy distributions of the emitted H atoms are shown in the top three histograms (a,b,c). One can see that the peak in the energy distribution near the incident energy (surface peak), which is present for Ti(c), disappears for TiH_2 (b). This is mainly a consequence of the increased nuclear stopping coming from the H atoms in TiH_2. For H ion energies in the range of 100 to 5 eV, the nuclear stopping cross section of a target H atom varies from 2 to 10 times larger than its electronic stopping cross section. The top left histogram (a) depicts the energy distribution of the sputtered H atoms. It is seen that the sputtered particles are less energetic than those reflected. The dashed line in the top center histogram (b) gives the combined energy distribution of the H sputtered and the H reflected. Histograms e and f give the maximum penetration depth reached by those particles that are later reflected and histogram d gives the depth at which the sputtered particles originate. Most of the sputtered particles are seen to originate near the surface. The bottom three histograms (g,h,i) of fig. 1 give the angular distribution of the emitted particles. The distributions are approximately cosine (dashed line).

Fig. 2 shows H reflection and sputtering for cases similar to fig. 1 except that here the incident H ion energy is 1.0 keV rather than 0.1 keV. The figure shows that the particle and energy reflection coefficients (R_N and R_E) of TiH_2 (b) are about 40% lower than of Ti (a). The dashed histogram (b) gives the total of both sputtered and reflected H. As in fig. 1, it is seen that the energies of the sputtered atoms are much less than the majority of those reflected. The sputtering yield, S_H, is now only about 40% of that found for 0.1 keV incident H ions (fig. 1, a). However, the average energy per sputtered particle is now about 50 eV whereas in fig. 1, it is less than 20 eV. Histogram d gives the energy distribution of H reflected from Ti for the case in which the electronic stopping has been arbitrarily doubled. The reflection coefficients are reduced by 30 to 40% compared with that for normal electronic stopping (a). The peak in the reflected particle energy distribution and the average energy of a reflected particle have both shifted to lower energy. The reflection features of Ti with an arbitrarily doubled electronic stopping are more similar to TiH_2 than to Ti with normal electronic stopping. This is not too surprising, as the two hydrogen target atoms contribute little to the backscattering, but contribute 85% as much electronic stopping as one Ti atom. Histograms d, e, and g give the maximum penetration depth of the particles reflected and are similar to those of fig. 1 except that here the depths are greater, corresponding to what one would expect with increased incident energy. Again it is seen that the sputtered particles originate at much shallower depths than those reflected. The angular distributions of the emitted particles are shown in the bottom four histograms (h, i, j, k). They approximate a cosine distribution (dashed line) fairly well.

The next three figures (3, 4, and 5) treat the reflection and sputtering of H from "iron hydrides" of varying hydrogen content. These target materials were chosen because of the current interest in the release of implanted hydrogen and deuterium from stainless steel[3,23]. It should be mentioned, however, that the computer results for TiH_2 and FeH_2 differ by only a few percent because of the closeness of the atomic number of Ti and Fe.

Fig. 3 shows the reflection and sputtering coefficients of H from FeH and FeH_2 for 100 and 500 eV H ions as a function of the angle of incidence. Both the particle and energy reflection coefficients, R_N and R_E, increase with increasing incident angle in a manner similar to that found for monatomic solids[15]. On the other hand, the H sputtering yield, S_N, and the fraction of incident energy sputtered, S_E, go through a maximum and then decrease as the angle of incidence is increased. The latter may be explained by the fact that at very large incident angles most of the incident particles are reflected from the surface and hence have little chance to sputter.

Fig. 4 shows the ratio of the hydrogen particle and energy reflection coefficients of "iron hydrides" with varying H content to the respective quantities of pure iron as a function of the incident H ion energy. It is seen that the reduction in both the particle number and energy reflected is independent of the incident energy in this energy region. Both the particle reflection ratio and the energy reflection ratio decrease monotonically as the H content increases. However, the reduction in the energy reflected is somewhat greater than the reduction in the particles reflected, showing that the average energy of those particles reflected decreases.

Fig. 5 compares H reflection and T sputtering from FeT with T reflection and H sputtering from FeH for normally incident ions of 100 and 500 eV. At each incident energy, both the particle and the energy reflection of H from FeT is greater than that of T from FeH. In contrast, both the sputtering yield and the fraction of incident energy carried away by the sputtered particles are several times larger for T incident on FeH than for H incident on FeT. The differences in the above results are mainly due to the factor of three difference in mass between tritium and hydrogen.

Discussion

An additional calculation that sheds light on the calculations presented above is the following. It is found that the reflection of H from solid H targets is very small (< 1%) for normally incident H ions of energies 0.1 to 1 keV. The amount of H sputtered is found to be more than an order of magnitude smaller than that from the "metal hydride" targets discussed earlier. These results show that H reflection is due to the metal atoms in the "metal hydrides" and that the H sputtering occurs mainly by the reflected ions as they exit through the surface layers and not by the incident ions as they enter. This latter result is not too surprising when one recognizes that the maximum in the nuclear stopping of H ions in H occurs at an energy of only about 30 eV. The above result concerning sputtering is for ions of normal incidence and would not be expected to be valid for angles of grazing incidence.

A cutoff energy of 5 eV was used in these computer simulation studies. It is found that the reflection coefficients are insensitive to the exact value used, provided it is at least several times larger than the incident energy. However, the sputtering results are sensitive to the cutoff energy. This is due to the fact that most of the H atoms are sputtered with low energies. This sensitivity to the cutoff energy should be kept in mind when using these calculations to interpret experiments. In each of the computer runs, the target composition remains constant, that is, no allowance is made for changes in H concentration in the target during the simulated ion bombardment. In reality, the H concentration builds up when the sum of the reflection and sputtering coefficients is less than one. The calculations show that the sum of the reflection and sputtering coefficients of FeH and of TiH_2 is less than one, indicating that neither target is H saturated. In contrast, it was found experimentally that the saturation concentrtion of H in Ti at room temperature is about 200%[24,25] and in Fe it is about 100% at liquid nitrogen temperature[26]. However, the sensitivity of the sputtering yield to the cutoff energy makes it hazardous to apply these calculations directly to the study of saturation.

In a recent experiment, Eckstein and Verbeek[19] have found the H reflection coefficient of TiH_2 to be 20% lower than that of Ti for normally incident H ions of 2.5 and 5 keV. On the other hand, computer simulations using MARLOWE predict a decrease of 40%. The reason for this factor of two difference between the calculations and experiment is not clear. One possible explanation is that the calculations assumed too large an electronic stopping cross section for the H target atoms. Above a few hundred eV, the electronic stopping dominates the nuclear stopping and, according to the LSS theory, two H atoms contribute 85% as much electronic stopping as one Ti atom.

Acknowledgements

One of the authors (OSO) would like to express his thanks to the members of the Plasma Wall Interactions group and to their director, H. Vernickel, for their kind hospitality during his stay in Garching. He also expresses thanks to R. Behrisch, W. Eckstein, and H. Verbeek for stimulating dicsussions.

REFERENCES

1. E. Hinnov, J. Nucl. Mater. 53 (1974) 9.
2. J. T. Hogan and J. F. Clarke, J. Nucl. Mater. 53 (1974) 1.
3. G. M. McCracken, S. J. Fielding, S. K. Erents, A. Pospieszczyk, and P. E. Stott, Nuclear Fusion 18 (1978) 35.
4. H. Verbeek, J. Appl. Phys. 46 (1975) 2981.
5. W. Eckstein, F. E. P. Matschke, and H. Verbeek, J. Nucl. Mater. 63 (1976) 199.
6. G. Sidenius and T. Lenskjaer, Nucl. Inst. Meth. 132 (1976) 673.
7. H. H. Andersen, T. Lenskjaer, G. Sidenius, and H. Sørensen, J. Appl. Phys. 47 (1976) 13.
8. H. Sørensen, in: Proc. Int. Symp. on Plasma Wall Interactions, Jülich, 1976 (Pergamon Press, Oxford, 1977) p. 437.
9. H. Sørensen, Appl. Phys. Lett. 29 (1976) 148.
10. J. E. Robinson and S. A. Agamy, presented at VII Int. Conf. on Atomic Collisions in Solids, Moscow, 1977.
11. S. Tanaka, Y. Murakami, and T. Shibata, Japan. J. Appl. Phys. 17 (1978) 183.
12. D. P. Jackson, presented at VII Int. Conf. on Atomic Collisions in Solids, Moscow, 1977.
13. J. E. Robinson, K. K. Kwok, and D. A. Thompson, Nucl. Inst. and Meth. 132 (1976) 667.
14. O. S. Oen and M. T. Robinson, J. Nucl. Mater. 63 (1976) 210.
15. O. S. Oen and M. T. Robinson, Nucl. Instr. Meth. 132 (1976) 647.
16. J. Vukanic and P. Sigmund, Appl. Phys. 11 (1976) 265.
17. U. Littmark and A. Gras-Marti, Fysisk Lab. II, H. C. Ørsted Inst., U. of Copenhagen, Monograph no. 78-04 (1978).
18. G. M. McCracken, in: Proc. Int. Symp. on Plasma Wall Interactions, Julich, 1976 (Pergamon Press, Oxford, 1977) p. 339.
19. W. Eckstein and H. Verbeek, in: Proceeding of this conference.
20. M. T. Robinson and I. M. Torrens, Phys. Rev. B9 (1974) 5008.

21. G. Molière, Z. Naturforsch. 2a (1947) 133.

22. J. Lindhard, M. Scharff, and H. E. Schiøtt, Kgl. Danske Videnskab. Selskab, Mat.-Fys. Medd. 33 no. 14 (1963).

23. R. S. Blewer, R. Behrisch, B. M. U. Scherzer, and R. Schulz, in: Proceedings of this conference.

24. J. Bohdansky, J. Roth, M. K. Sinha, W. Ottenberger, J. Nucl. Mat. 63 (1976) 115.

25. E. S. Hotston, G. M. McCracken, J. Nucl. Mat. 68 (1977) 277.

26. C. J. Altstetter, R. Behrisch, and B. M. U. Scherzer, J. Vac. Sci. Tech. (to be published).

FIGURE CAPTIONS

Fig. 1

Energy, maximum penetration depth and angular distribution of H reflected from Ti and TiH_2 for normally incident H ions. For TiH_2 the energy, depth of origin, and angular distribution of the H sputtered are shown. The ordinate gives the number of particles reflected or sputtered in each histogram channel. The dashed line in histogram b gives the combined total of reflected and sputtered particles. The dashed sloped line in each of the angular plots is a cosine distribution shown for comparison.

Fig. 2

Energy, maximum penetration depth and angular distribution of H reflected from Ti, TiH_2 and Ti (doubled electronic stopping) for normally incident H ions. For TiH_2 the energy, depth of origin and the angular distribution of the sputtered H are shown. The ordinate gives the number of particles reflected or sputtered in each histogram channel. The dashed line in b gives the combined reflected and sputtered particles. The dashed line in the angular plots is a cosine distribution for comparison.

Fig. 3

Particle and energy reflection coefficients and sputtering yield (S_n) and the fraction of incident energy carried by sputtered particles (S_E) as functions of the angle (measured from surface normal) of the incident beam.

Fig. 4

Ratio of the hydrogen particle and energy reflected from "iron hydrides" to those quantities from pure iron as a function of the incident H energy (normal incidence). The error bars represent the standard deviations of the values plotted based on the Monté Carlo calculations.

Fig. 5

Energy distributions of H reflected from FeT, T reflected from FeH, T sputtered from FeT and H sputtered from FeH for normally incident ions. The distribution of the depth of origin of the sputtered particles is also shown. The ordinate gives the number of particles reflected or sputtered in each histogram channel.

100 eV H ATOMS INCIDENT UPON Ti AND TiH$_2$

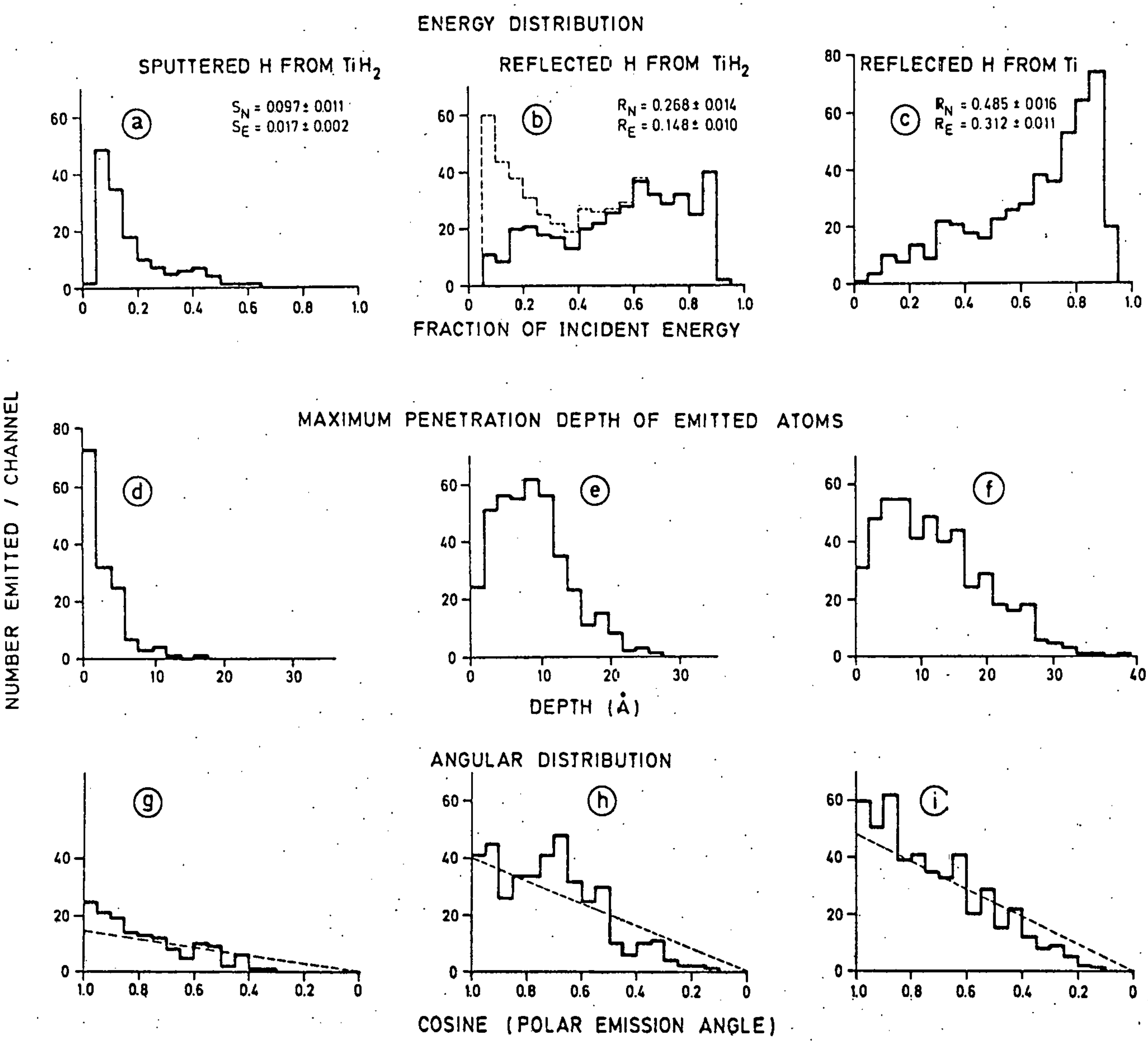

Fig. 1

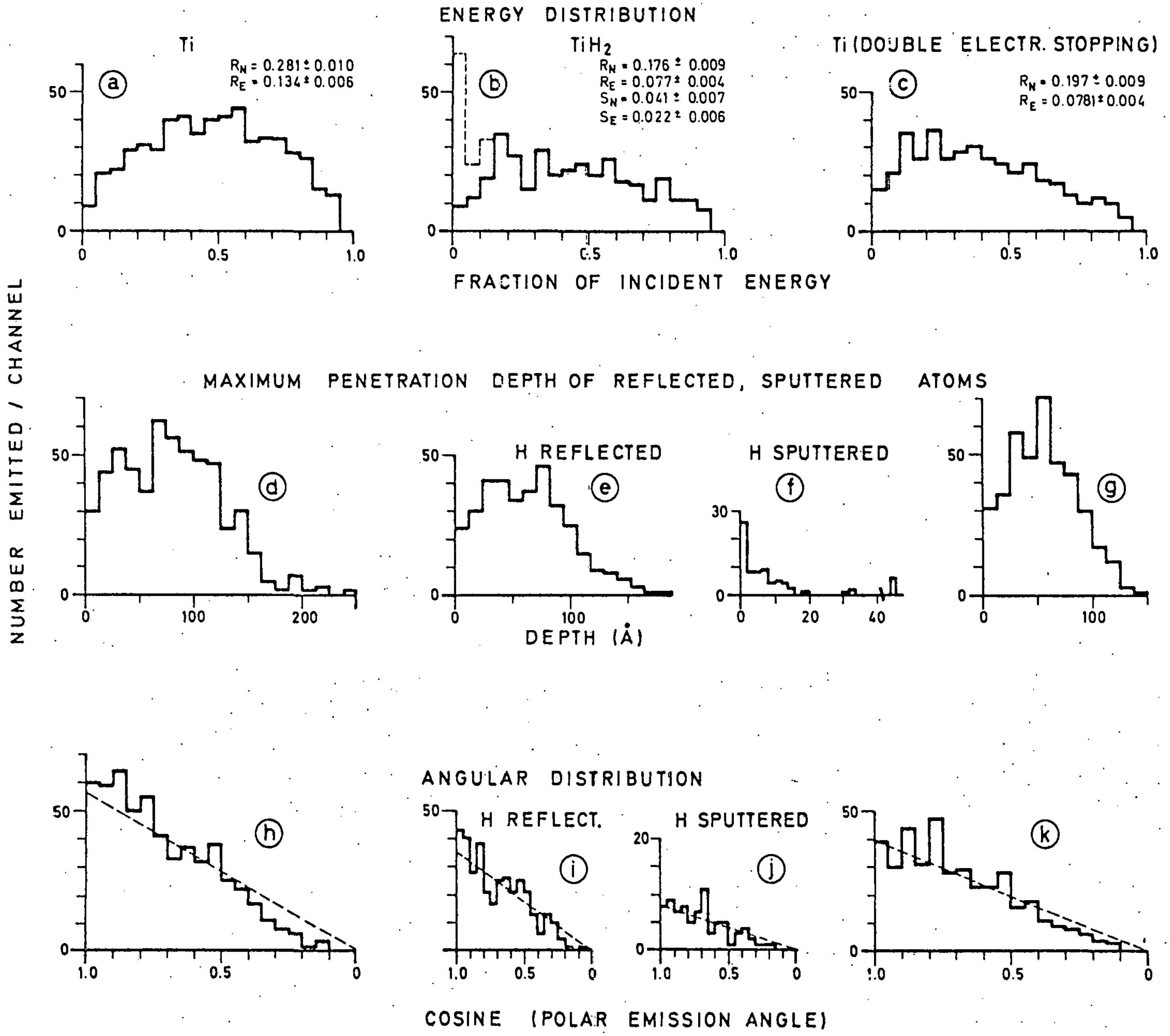
ENERGY DISTRIBUTION
Ti
TiH$_2$
Ti (DOUBLE ELECTR. STOPPING)
ⓐ
$R_N = 0.281 \pm 0.010$
$R_E = 0.134 \pm 0.006$
ⓑ
$R_N = 0.176 \pm 0.009$
$R_E = 0.077 \pm 0.004$
$S_N = 0.041 \pm 0.007$
$S_E = 0.022 \pm 0.006$
ⓒ
$R_N = 0.197 \pm 0.009$
$R_E = 0.0781 \pm 0.004$
0
50
0
0.5
1.0
FRACTION OF INCIDENT ENERGY
NUMBER EMITTED / CHANNEL
MAXIMUM PENETRATION DEPTH OF REFLECTED, SPUTTERED ATOMS
ⓓ
H REFLECTED
ⓔ
H SPUTTERED
ⓕ
ⓖ
30
100
200
20
40
DEPTH (Å)
ANGULAR DISTRIBUTION
ⓗ
H REFLECT.
ⓘ
H SPUTTERED
ⓙ
ⓚ
COSINE (POLAR EMISSION ANGLE)

Fig. 2

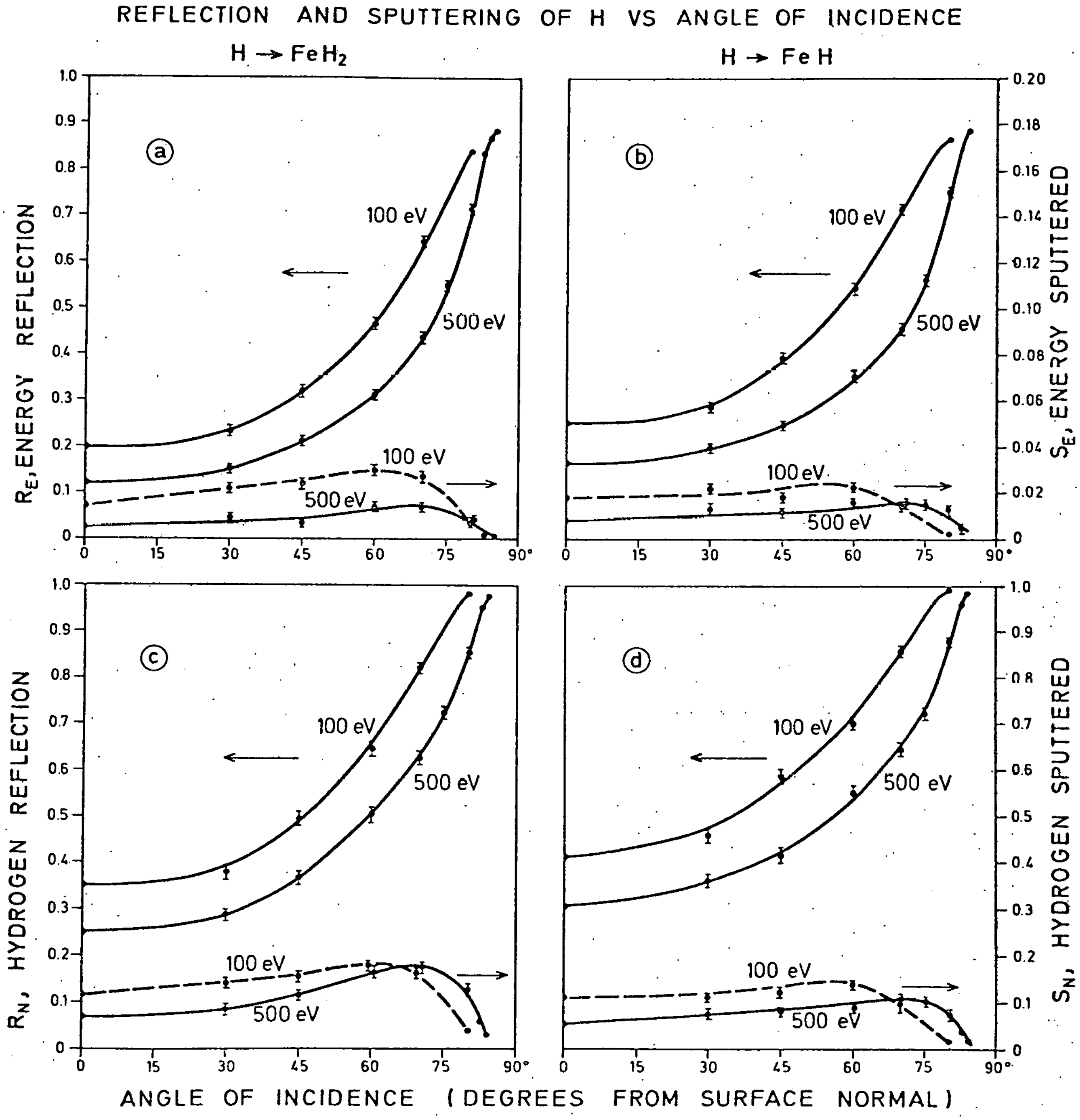
REFLECTION AND SPUTTERING OF H VS ANGLE OF INCIDENCE
H → FeH₂
H → FeH
ⓐ
ⓑ
ⓒ
ⓓ
100 eV
500 eV
R_E, ENERGY REFLECTION
S_E, ENERGY SPUTTERED
R_N, HYDROGEN REFLECTION
S_N, HYDROGEN SPUTTERED
0
0.1
0.2
0.3
0.4
0.5
0.6
0.7
0.8
0.9
1.0
0.02
0.04
0.06
0.08
0.10
0.12
0.14
0.16
0.18
0.20
0
15
30
45
60
75
90°
ANGLE OF INCIDENCE (DEGREES FROM SURFACE NORMAL)

Fig. 3

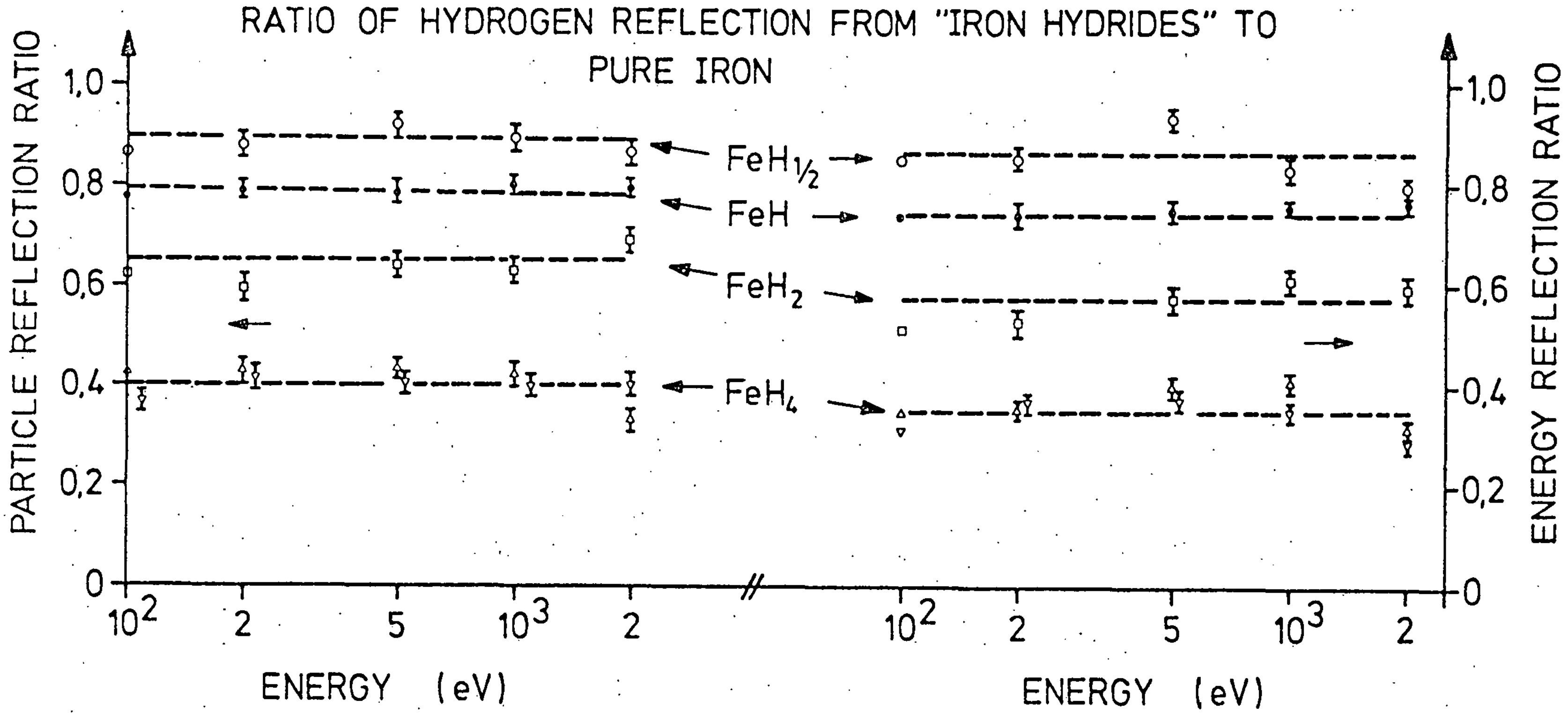
RATIO OF HYDROGEN REFLECTION FROM "IRON HYDRIDES" TO PURE IRON
PARTICLE REFLECTION RATIO
ENERGY REFLECTION RATIO
1,0
0,8
0,6
0,4
0,2
0
$FeH_{1/2}$
FeH
FeH_2
FeH_4
10^2
2
5
10^3
2
ENERGY (eV)
ENERGY (eV)

Fig. 4

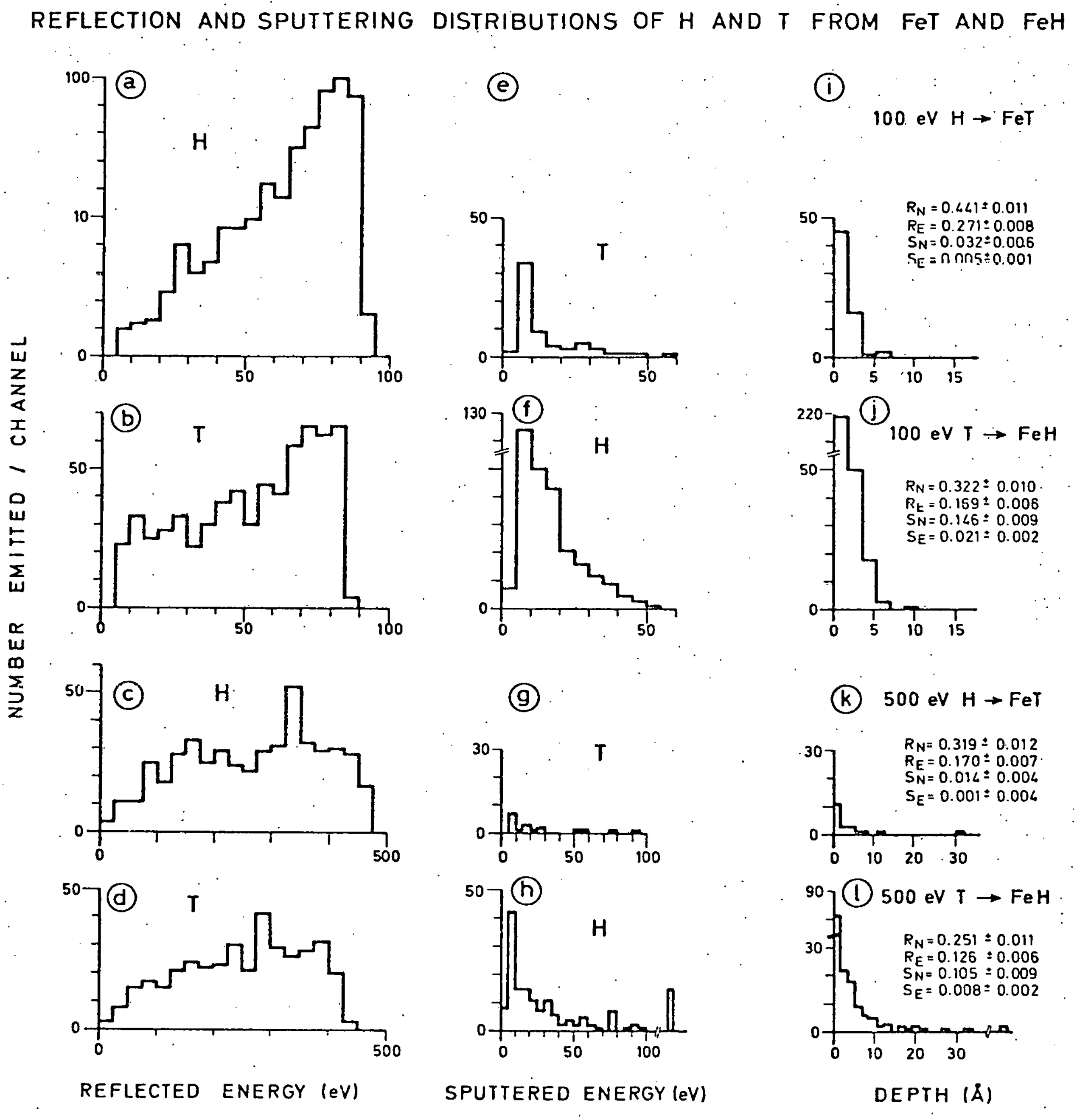
REFLECTION AND SPUTTERING DISTRIBUTIONS OF H AND T FROM FeT AND FeH
NUMBER EMITTED / CHANNEL
(a) H
100
10
0
0 50 100
(b) T
50
0
0 50 100
(c) H
50
0
0 500
(d) T
50
0
0 500
REFLECTED ENERGY (eV)
(e) T
50
0
0 50
(f) H
130
0
0 50
(g) T
30
0
0 50 100
(h) H
50
0
0 50 100
SPUTTERED ENERGY (eV)
(i) 100 eV H → FeT
$R_N = 0.441 \pm 0.011$
$R_E = 0.271 \pm 0.008$
$S_N = 0.032 \pm 0.006$
$S_E = 0.005 \pm 0.001$
50
0
0 5 10 15
(j) 100 eV T → FeH
$R_N = 0.322 \pm 0.010$
$R_E = 0.169 \pm 0.006$
$S_N = 0.146 \pm 0.009$
$S_E = 0.021 \pm 0.002$
220
50
0
0 5 10 15
(k) 500 eV H → FeT
$R_N = 0.319 \pm 0.012$
$R_E = 0.170 \pm 0.007$
$S_N = 0.014 \pm 0.004$
$S_E = 0.001 \pm 0.004$
30
0
0 10 20 30
(l) 500 eV T → FeH
$R_N = 0.251 \pm 0.011$
$R_E = 0.126 \pm 0.006$
$S_N = 0.105 \pm 0.009$
$S_E = 0.008 \pm 0.002$
90
30
0
0 10 20 30
DEPTH (Å)

Fig. 5